

HYDROCONVERSION OF HEPTANE CATALYZED BY SULFIDED NiMo/HY ZEOLITES*

Jacques LEGLISE, Mohammed EL QOTBI and Daniel CORNET

"Catalyse et Spectrochimie", URA CNRS 04414, I.S.M.Ra.,

Université de Caen, 14050 Caen Cedex, France

Received September 13, 1991

Accepted October 22, 1991

A series of catalysts made of Ni, Mo and NiMo sulfide encaged in HY zeolites ($\text{Si}/\text{Al} = 3$ to 17) were tested for the hydroconversion of heptane. The reaction was carried out at $P(\text{H}_2) = 8$ MPa and with a constant supply of H_2S . Propane and isobutane were the main products, but bimolecular cracking processes occurred to some extent. The yield of heptane isomers was low, showing a deficient hydrogenation function. The influence of the Si/Al ratio upon catalytic activity and selectivity was examined.

The transformation of heptane into cracked products and C_7 isomers constitutes a valuable test of the activity and selectivity of hydrocracking catalyst. Catalysts such as Pt or Pd supported on acidic zeolites were examined in this way¹⁻⁴, and the maximum amount of isomers varied between 10 and 70% according to the metal loading, or the geometry of the zeolite pores. The test is thus sensitive to the balance between the acidic and the hydrogenation function.

In recent catalysts, NiMo or NiW sulfides have been substituted for the noble metal⁵⁻⁷, but their lower hydrogenation activity makes them obviously very different from the Pt or Pd/zeolites. In this work, the heptane conversion was carried out under a high pressure of hydrogen in order to evaluate the properties, mainly the stability and the selectivity, of some zeolites containing a Ni, Mo or NiMo sulfide. The feed also contained a small amount of dimethyl disulfide (DMDS), and 20% benzene. In this way, the rate of hydrogenation of benzene afforded an independent measure of the hydrogenation function^{8,9}. Several HY zeolites with Si/Al ratios ranging from 3 to 17 were used as supports, so that the number of acid sites varied in a broad range.

EXPERIMENTAL

Catalysts. The HY-3 support was the commercial Linde LZY-82, with an overall Si/Al ratio equal to 3. HY zeolites with $\text{Si}/\text{Al} = 3.9$, 5.3 and 17 were prepared by steaming an ammonium

* Presented as a poster at the *International Symposium "Zeolite Chemistry and Catalysis"*, Prague, September 8-13, 1991.

exchanged NaY zeolite (Linde LZY-52) and washing the resulting material with a 1M HCl solution.

The HY supports were ion-exchanged or impregnated with a nickel acetate solution, then molybdenum was added by dry impregnation with an ammonium heptamolybdate solution. The catalyst names (e.g. NiMo-3) recall both the metal introduced, and the overall Si/Al ratio of the zeolite support.

The composition of the catalysts is given in Table I, together with the BET areas and pore volumes deduced from the N_2 isotherms. A comparison with NH_4Y ($S_{BET} = 729 \text{ m}^2 \text{ g}^{-1}$ and $V_{tot} = 0.379 \text{ cm}^3 \text{ g}^{-1}$) shows that the dealuminated zeolites remain highly crystalline but mesopores are created by the acid leaching.

Apparatus and procedure. The vertical stainless steel reactor (12 mm i.d.), containing 0.16 g of the calcined catalyst diluted with carborundum, operated under a hydrogen pressure of 8 MPa. The standard sulfidation procedure was as follows: the reactor temperature being set at 373 K, a mixture of heptane (78 wt. %), benzene (20%) and DMDS (2%) was fed by means of a liquid pump at a rate of 0.2 ml h⁻¹. The liquid was instantly vaporized when mixed with the hydrogen flow and DMDS was fully decomposed above 500 K, so that the H₂/H₂S ratio in the inlet gas was 4.100 mol/mol. The temperature of the reactor was slowly raised up to 593 K, and the final temperature was maintained for one day in order to stabilize the sulfur content of the catalyst.

In a few cases (sulfidation A), the catalyst was presulfidized under a H₂ + H₂S flow (90 : 10) up to 623 K and at atmospheric pressure, then cooled down and the high pressure sulfidation was started.

The reaction products were analysed by on-line gas chromatography, using a OV 1701 capillary column. Since slow variations in pump speed led to some uncertainty in the actual feed rates of heptane and benzene, the instantaneous partial pressures of all hydrocarbons were deduced

TABLE I
Composition and texture properties of the catalysts (oxide state); degree of sulfidation and numbers of acid sites (sulfide state)

Catalyst	NiO wt. %	MoO ₃ wt. %	S_{BET} $\text{m}^2 \text{ g}^{-1}$	Pore volume $\text{cm}^3 \text{ g}^{-1}$		Degree of sulfida- tion ^a	IR band intensities ^b	
				total	micro		Brønsted Py	Lewis Py
HY-3	0	0	541	0.346	0.233	—	100	100
Ni-3	4.25	0	637	0.372	0.273	0.71	100	22
Mo-3	0	12.1	502	0.304	0.211	0.26	61	91
NiMo(a)-3	3.5	13.6	449	0.277	0.196	0.48	81	15
NiMo(b)-3	3.5	6.8	472	0.292	0.213	0.36	—	—
NiMo-3-9	2.0	12.9	501	0.360	0.213	0.45	37	31
NiMo-5-3	3.8	12.4	526	0.411	0.223	0.54	33	26
NiMo-17	2.8	14.7	518	0.417	0.216	0.48	19	22

^a DS = S / (0.66 Ni + 2 Mo) molar ratio. ^b Relative intensities of the 1 545 and 1 455 cm^{-1} bands for pyridine adsorbed at 150°C.

from the intensities of the GLC peaks. From these, and the known hydrogen flow rate ($0.25 \text{ mol} \cdot \text{h}^{-1}$), the feed rates $F(\text{Hp})$ and $F(\text{Be})$ were determined more accurately: they could differ by $\pm 30\%$ from their nominal values, $1.1 \cdot 10^{-3}$ and $0.36 \cdot 10^{-3} \text{ mol h}^{-1}$, respectively. Good mass balances could be established over periods of 12 h.

Since benzene hydrogenation follows a zero order⁸, the conversions had to be normalized to the nominal $F(\text{Be})$ value. No such correction was necessary for the conversion of heptane which is nearly first order in this pressure range¹⁰.

RESULTS AND DISCUSSION

Sulfidation and Stabilization of the Catalysts

The simultaneous conversion of heptane and benzene over the NiMo/HY catalysts yielded the three kinds of expected products. Heptane was converted into C_7 isomers (conversion x_{iso}) or light alkanes $\text{C}_1 - \text{C}_6$ (x_{cra}), and benzene was hydrogenated into methylcyclopentane (MCP) and cyclohexane (CHX), the total yield being x_{hyd} . Toluene and C_8 aromatics were also detected, showing that benzene could be alkylated by the small amount of DMDS present in the feed. Heptane reacted 10 to 20 times faster than benzene over all catalysts, and gave mainly cracked products. Hence, any secondary products arising from the transformation of benzene might be neglected, and the whole of the $\text{C}_2 - \text{C}_6$ was ascribed to the transformation of heptane.

As the catalyst was sulfided at increasing temperature by the DMDS-containing feed, a stable activity level was reached only after 15 h at the upper temperature (593 K). Figure 1 shows the evolution of the conversions x_{iso} , x_{cra} and x_{hyd} for two

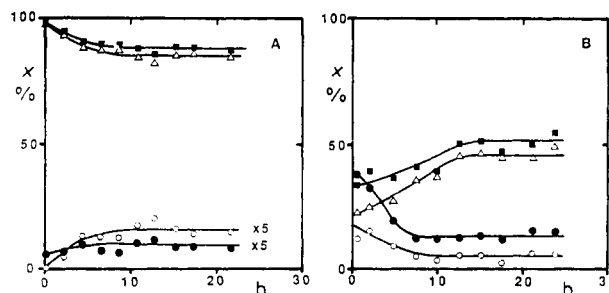


FIG. 1

Conversion of heptane and benzene versus time-on-stream at 593 K ($\text{Hp} + \text{Be}$ feed = $0.143 \text{ g} \cdot \text{h}^{-1}$). A: $0.16 \text{ g NiMo(b)/HY-3}$; B: $0.32 \text{ g NiMo/HY-17}$. Conversion of heptane: ■ x_{tot} ; △ x_{cra} ; ○ x_{iso} . Conversion of benzene: ● x_{hyd}

NiMo catalysts during the final isotherm. The overall conversion of heptane as well as x_{cra} initially decreased over catalyst NiMo(b)-3, but increased over NiMo-17. The conversion of benzene into MCP and CHX varied in a way opposite to x_{cra} , and interestingly, the yield of heptane isomers varied in accordance with benzene hydrogenation.

Thus, the sulfureduction of the Ni and Mo ions depends somewhat on the nature and possibly the texture of the zeolite support. A maximum in x_{hyd} is noted for catalyst NiMo-17 at the end of the temperature ramp. No such maximum appears with the catalyst NiMo-3, whose support had not been washed with HCl and thus contains a lot of amorphous alumina. In the former case, intermediate reduction of Ni^{2+} into Ni^0 is a possibility, whereas direct sulfidation would occur with the HY-3 support.

The sulfur contents of the catalysts were rather low in any case. The sulfidation degrees (DS) shown in Table I were based on the assumption that full sulfidation would produce Ni_3S_2 and MoS_2 , as with $\text{NiMo}/\text{Al}_2\text{O}_3$ catalysts¹¹. The degree of sulfidation of the NiMo catalysts ranges from 36 to 54%, and there is no obvious correlation with the zeolite structure or composition. Thus the low sulfur content is inherent to the zeolite support¹², rather than to the high $\text{H}_2/\text{H}_2\text{S}$ ratio.

In accordance with this, similar sulfur contents were found for catalyst NiMo(a)-3 sulfided at high pressure (DS = 48%) or according to process A (DS = 43%). Yet, the latter catalyst converts much less heptane. As can be seen in Fig. 2, the activity curve of catalyst NiMo(a)-3 is shifted 35 K upwards when performing sulfidation A (at 623 K and 0.1 MPa) instead of the standard high pressure sulfidation. The maximum in isomer yield x_{iso} is also depressed from 12 to 3.5%. The eight-fold decrease in hydrocracking activity is quite surprising since the rate of benzene hydrogenation measured at 553 K only dropped⁹ from $48 \cdot 10^{-3}$ to $33 \cdot 10^{-3}$ mol $\cdot \text{h}^{-1} \text{kg}^{-1}$. Thus, the hydrogenation function is not much lower after sulfidation A.

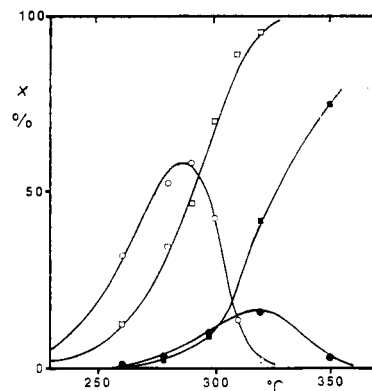


FIG. 2

Conversion of heptane versus temperature over NiMo(a)/HY-3. Catalyst weight 0.16 g; $\text{H}_2 + \text{Be}$ feed = 0.143 g h^{-1} . High pressure sulfidation: ■ x_{tot} ; ● $x_{\text{iso}} \times 5$. Low pressure sulfidation: □ x_{tot} ; ○ $x_{\text{iso}} \times 5$

Therefore, the activated procedure strongly affects the acidic function. This was confirmed by measuring the rate of benzene alkylation, which is an acid-catalyzed reaction. The amount of alkylbenzenes formed at 553 K was much lower on the A-sulfided catalyst (<0.1% instead of 9.3% for the standard treatment).

In any case, sulfiding the catalyst by the feed proved satisfactory with respect to activity and stability. The only exception was Ni-3, which was rapidly deactivated by coke deposition. Over this catalyst, the hydrogenation function was obviously unsufficient.

Selectivity in Heptane Conversion

All MS/HY catalysts exhibited a number of common features in the hydroconversion of heptane. The catalytic test was carried out with the Hp + Be feed, but pure

TABLE II

Reaction of heptane (Hp) at 553 K. Influence of catalyst sulfidation and of benzene (Be) in the feed upon selectivity for C₇ isomers (mole %) and for cracked products (mol/100 mol C₇ cracked)

Catalyst	NiMo(a)/ HY-3	NiMo(a)/HY-3 ^a		NiMo/HY-17		
Feed	Hp + Be	Hp + Be	Hp	Hp + Be	Hp + Be	Hp
Catal. weight, g	0.16	0.16	0.16	0.16	0.54	0.54
<i>x</i> _{tot} , %	34.9	2.25	4.0	4.0	65.3	92.3
Isomers, <i>x</i> _{iso} , wt.%	10.5	0.75	1.7	1.5	12.6	1.8
2-MH + 3-MH	74.5	78.5	73.8	77.2	72.9	72.6
3-EP	3.3	0.8	2.3	3.4	2.0	0.8
2,3 + 2,4-DMP	20.8	19.7	22.0	17.1	22.3	24.0
2,2 + 3,3-DMP	1.4	1.0	1.9	2.3	2.8	2.6
Cracking, <i>x</i> _{cra} , %	24.4	1.5	2.3	2.5	52.7	90.5
C ₃	87.1	90.7	90.1	89.6	88.3	85.4
i-C ₄	87.7	89.1	85.9	85.8	87.1	84.8
n-C ₄	7.9	11.4	12.8	7.1	8.1	8.5
i-C ₅	5.4	2.8	4.4	5.7	4.7	6.8
n-C ₅	0.4	0.3	0.8	0.2	0.5	1.0
C ₆	2.2	<0.5	<0.5	3.0	2.6	4.1
Total <i>N</i> _{cra}	190.7	194.3	194.0	191.4	191.4	190.6

^a Catalyst presulfided at 623 K and 0.1 MPa.

heptane was also run in a few cases. It could be established that benzene had no measurable influence on the product distribution or the selectivity (Table II) and only lowered the overall rate of C_7 conversion by about 50%.

Overall selectivity. In principle, the conversions represented in the selectivity diagram (x_{iso} vs x_{cra}) should be recorded at a constant temperature. In practice, however, the various conversion levels are most easily obtained at different temperatures, the flow rate being kept constant.

Figure 3 represents such a diagram for a typical catalyst NiMo(b)-3. The C_7 isomers clearly appeared as primary products, but x_{iso} never exceeded 11.5%. The relative amounts of mono and dibranched (MB and DB) isomers did not vary much with overall conversion (Fig. 4). Up to 90% conversion, the quantities of 2- and 3-methylhexanes were higher than allowed by thermodynamics (dashed lines on Fig. 4). In the dibranched fraction, the most abundant isomer, the 2,3-dimethylpentane was well under its equilibrium value, and the 2,2- and 3,3-DMP were produced in small amounts. The 2,2,3-trimethylbutane reached only 0.2% of the C_7 isomers.

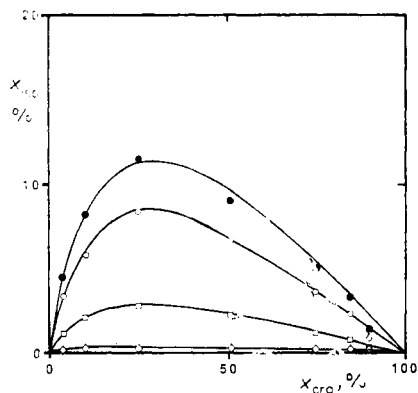


FIG. 3

Selectivity in heptane hydroconversion over NiMo(b)/HY-3 at various temperatures: yield of C_7 isomers versus % heptane cracked.
 ● Total isomers; ○ monobranched; dibranched: □ 2,3- and 2,4-dimethylpentanes;
 ◇ 2,2- and 3,3-dimethylpentanes

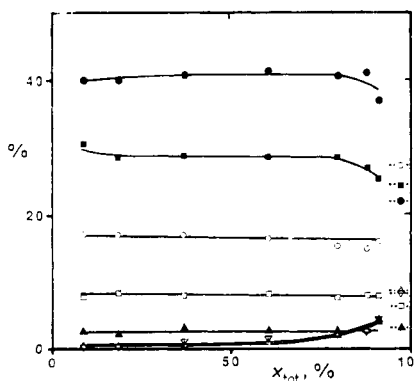
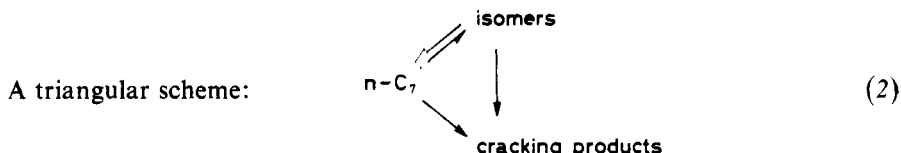


FIG. 4

Selectivity in heptane hydroisomerization over NiMo(b)/HY-3 at various temperatures: distribution of C_7 isomers versus overall heptane conversion. (Thermodynamic values at 327°C are given on the right). Monobranched: ● 3-methylhexane; ■ 2-methylhexane; ▲ ethylpentane. Dibranched: ○ 2,3-dimethylpentane; □ 2,4-dimethylpentane; △ 2,2-dimethylpentane; ▽ 3,3-dimethylpentane

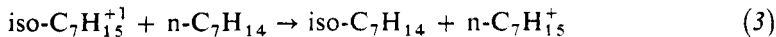
These results agree with a bifunctional mechanism, in which carbenium ions undergo isomerization prior to cracking. With this mechanism, however, several kinetic networks can be observed^{4,13,14}. Since the mono- and dibranched isomers do not appear successively, only two simple schemes, based on three groups of lumped species, may be considered here.

A consecutive scheme: $n\text{-C}_7 \rightleftharpoons \text{isomers (MB} \rightleftharpoons \text{DB}) \rightarrow \text{cracking products}$ (1)



Assuming that all reactions are first order and have the same activation energy¹⁴, the selectivity curve can be modeled in either scheme. The various rate constants may thus be deduced from the experimental points by means of a regression. On any of the metal sulfide/zeolite (MeS/HY) catalysts, the selectivity curve was best fitted with the triangular scheme (2). In a few cases however, notably for the more active NiMo catalysts, the value of the rate constant for direct cracking was not significant with respect to statistical criteria.

Nevertheless, the apparent reaction scheme indicates that the desorption of C_7 isomers by hydrogen transfer with an alkene, viz.



is not much faster than the cracking of the branched carbenium ion, probably because the concentration of olefins near the acidic sites is rather low.

Selectivity among C_7 isomers. Although the yield of C_7 isomers was much lower on the MeS/HY than on the Pt/zeolite catalysts, their internal distributions were not so different. Figures 3 and 4 show that, over the NiMo(b)-3 catalyst, the mono-branched isomers amounted up to 78%, as with a 1% Pt/USY (ref.²). For Pt/HY catalysts with Pt content ranging from 0.1 to 1%, the selectivity for monobranched isomers varied from 73 to 80% (ref.¹³), but a value as high as 94% was reported for a reduced NiMo/HY catalyst¹⁵.

More significantly, the quantities of 2,2- and 3,3-dimethylpentanes never exceeded 2% over the MeS/HY catalyst, except at very high conversion. This is much lower than the 6.4% quoted for Pt/USY (ref.²) or 10.5% for Pt/HY (ref.¹³). Since carbenium ions with a quaternary carbon are formed by a succession of isomerization steps, this is a further proof that over the MeS/HY catalysts, desorption of these ions is not much faster than their splitting.

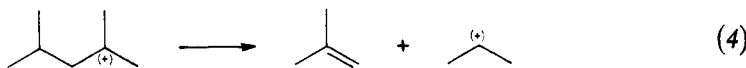
Furthermore, the ratio r between 2- and 3-methylpentane was examined, since it is very sensitive to the mechanism of carbenium ion isomerization¹⁶: the alkyl shift mechanism predicts $r = 1$, and the cyclic intermediate (PCP) mechanism $r = 0.5$. Over Pt/zeolites, r is found nearly unity, and hardly goes below 0.9 at low conversion^{4,16}. With the MeS/HY, and over a wide range of conversions, r was found equal to 0.7, which is closer to the value of the PCP mechanism. Therefore, the PCP mechanism appears important with those catalysts.

Cracking Selectivity

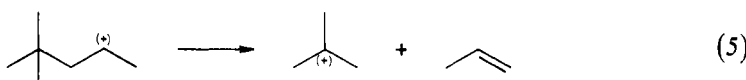
Table II shows some distributions of cracked products observed with catalysts NiMo(a)-3 and NiMo-17 at various conversion levels. They are expressed as moles $C_n/100$ moles C_7 cracked, and N_{cra} represents the sum of the cracked moles. C_1 and C_2 are not recorded here, but separate determinations have shown that the observed C_1 corresponds very nearly to the decomposition of DMDS, and C_2 is less than one sixth of the amount of C_5 .

Propane and isobutane were the main cracking products (Table II and Fig. 5), accounting for 88% of the C_7 cracked. The other products were butane, pentanes and hexanes. This pattern strongly deviates from the ideal hydrocracking. For instance, a 1% Pt/USY catalyst operated at 473 K yielded only propane and isobutane, in equal amounts², and the small amounts of C_1 , C_2 , C_5 and C_6 observed at higher temperatures were attributed to metal-catalyzed hydrogenolysis^{1,16}. Furthermore, the values of N_{cra} reported in Table III did not exceed 191, instead of 200 if single splitting of carbenium ions had occurred. The discrepancy is much larger than the C_2 neglected in computing N_{cra} .

Yet, the main cracking route appears to be the β -splitting of branched $C_7^{(+)}$ carbenium ions. The modes to be considered² are: B_1 (sec \rightarrow tert-carbenium), B_2 (tert \rightarrow sec) and C (sec \rightarrow sec). Isobutane and propane arise mainly from the B_1 splitting of a 2,4-dimethylpentyl ion.

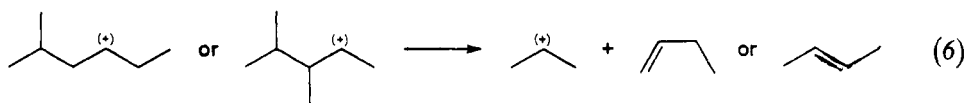


The B_2 splitting of the 2,2-dimethylpentyl ion:

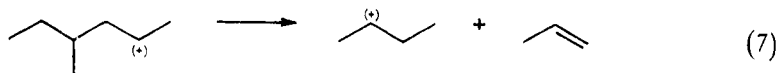


would give the same final products. But the amount of 2,2-dimethylpentane is very small, and comparable to that of 3,3-dimethylpentane which cannot be cracked. Thus, the above reaction is probably unimportant.

The normal butane, which appeared as an initial product in all distributions (Fig. 5), may arise from three different C-mode splittings.



and



The above mechanisms however fail to explain the observed amounts of butanes and propane, with $C_4 > C_3$, as well as the appearance of C_5 and C_6 at all conversions. From Figs 5 and 6, it is clear that most of the C_5 and C_6 are initial products. As C_1 and C_2 are virtually absent, the $C_5 - C_6$ cannot be formed by hydrogenolysis of heptane. They likely arise from the β -splitting of carbenium ions larger than C_7 . Such heavy ions are produced by bimolecular reactions¹⁷.

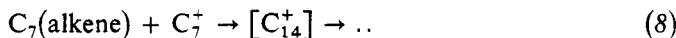


TABLE III

Structural data, apparent activation energy $E_a(\pm 8 \text{ kJ mol}^{-1})$ and turnover frequency (TOF) for the conversion of heptane over the metal sulfide/HY catalysts; (Hp + Be) feed

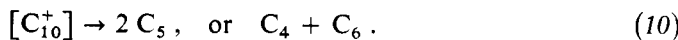
Catalyst	Al(F) atoms/ u.c.	Al(EF) Al(total) %	E_a kJ mol^{-1}	k_{HYC} at 553 K $\text{mol h}^{-1} \text{kg}^{-1}$ MPa^{-1}	TOF $\text{h}^{-1} \text{MPa}^{-1}$
HY-3	32	40	—	—	—
Ni-3	30	44	146	2.0	0.9
Mo-3	30	44	204	21	10
NiMo(a)-3	29	47	139	68	37
—	—	—	189 ^a	3.5	—
NiMo(b)-3	29	47	137	81	41
NiMo-3.9	15	66	153	62	63
NiMo-5.3	13	61	129	70	81
NiMo-17	3.5	68	115	6.6	27

^a Catalyst presulfidized at 623 K and 0.1 MPa.

Two successive splittings may then occur, giving fragments with at least six carbons, e.g.:



then



The cracking of the C_8 to C_{11} carbenium ions produces a low amount of propane, so that the observed distributions are qualitatively explained. A simple calculation, based on the cracking patterns of the C_8 – C_{11} alkanes², yields a 1/3 probability for the splitting of the C_6 fragment, and shows that the bimolecular mechanism accounts

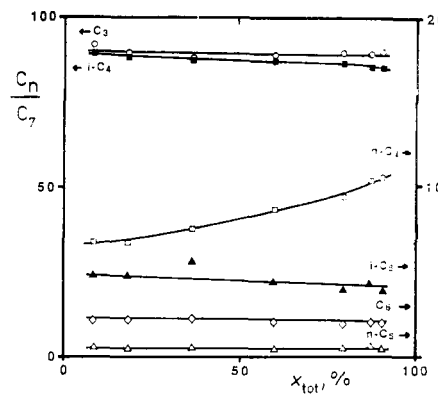


FIG. 5

Hydrocracking of heptane over NiMo(b)/HY-3 at various temperatures: number of moles C_n formed per 100 mol C_7 cracked, versus overall heptane conversion. \circ C_3 ; \blacksquare $i\text{-}C_4$; \square $n\text{-}C_4$; \blacktriangle $i\text{-}C_5$; \triangle $n\text{-}C_5$; \diamond C_6

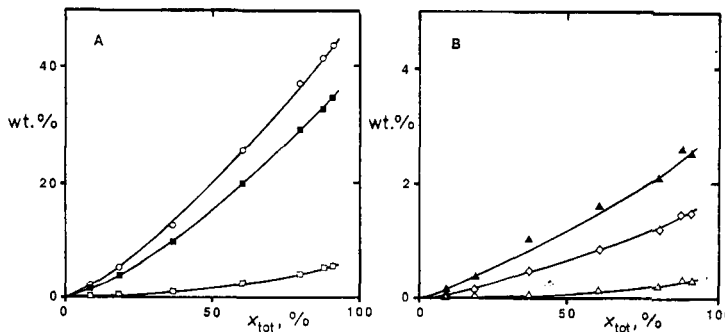


FIG. 6

Hydrocracking of heptane over NiMo(b)/HY-3 at various temperatures: yield (wt. %) of individual cracked products versus overall heptane conversion. A: \circ C_3 , \blacksquare $i\text{-}C_4$, \square $n\text{-}C_4$; B: \blacktriangle $i\text{-}C_5$, \triangle $n\text{-}C_5$, \diamond C_6

for 13% of the overall reaction. Although the products of heptane cracking are fairly well modeled, the calculated N_{cra} stays too high, showing that the bimolecular processes are likely to be repetitive.

Bimolecular cracking processes appear over bifunctional catalysts when the hydrogenation function is not in line with the acidic function¹⁸, i.e. whenever the concentration of alkene in the vicinity of the acidic centers is too low. They are then related to the slow desorption of alkane isomers. As shown by the nearly constant amounts of C₅ and C₆ (Fig. 6), their importance did not vary much with temperature, at least between 533 and 593 K.

Finally, the ratios n/iso in every cracked fraction increased with temperature, and the effect was more pronounced in the C₄ fraction. This is attributed to mechanism C, which becomes increasingly important compared to B₁. But the ratio n-C₄/i-C₄ always stands below thermodynamics, so that a secondary isomerization of isobutane at high conversion is not excluded.

Comparison of the Catalysts

Comparison of activities. The overall conversions of heptane measured with the heptane + benzene (Hp + Be) feed over five NiMo zeolites are shown in Fig. 7. The three catalysts NiMo(a)-3, NiMo(b)-3, and NiMo-5·3 appeared nearly equi-

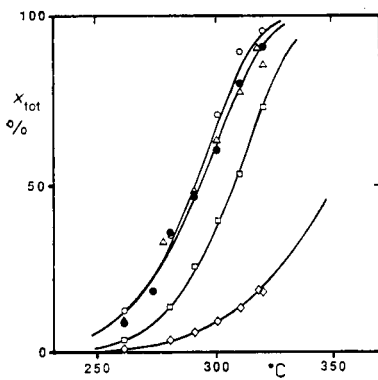


FIG. 7

Influence of catalyst structure upon conversion of heptane at various temperatures over
 ○ NiMo(a)/HY-3, ● NiMo(b)/HY-3, □ NiMo/HY-3·9, △ NiMo/HY-5·3 and ◇ NiMo/HY-17. Catalyst weight 0·16 g;
 (Hp + Be) feed = 0·143 g h⁻¹

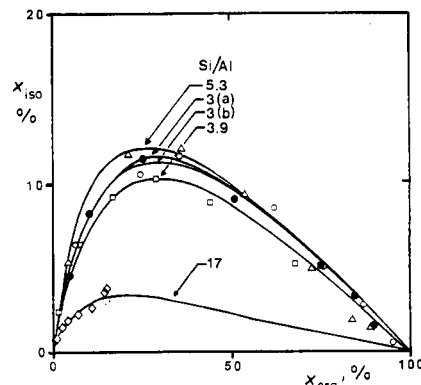


FIG. 8

Selectivity of heptane hydroconversion (x_{iso} versus x_{cra}) over catalysts ○ NiMo(a)/HY-3,
 ● NiMo(b)/HY-3, □ NiMo/HY-3·9, △ NiMo/HY-5·3, ◇ NiMo/HY-17

valent, as all activity points fit the same curve. The NiMo-3·9 was slightly less active, the NiMo-17 considerably less. The apparent activation energies deduced from these curves were all near 135 kJ mol^{-1} (Table III). A similar value has been reported for the conversion of pure heptane over an industrial NiMo catalyst¹⁰. The activation energy is the same whether benzene is present or not: this was verified for the NiMo(a)-3 catalyst. Higher activation energies, about 190 kJ mol^{-1} , were found over the Mo-3 and also with the NiMo-3 presulfided at atmospheric pressure. But these catalysts were less active and had to be tested at higher temperatures: the increased activation energy measured under these conditions may reflect modifications of the surface, such as those occurring with ammonia¹⁰. Thus, the variations in activity of the MeS/HY catalysts were not clearly related with variations in activation energy.

Selectivity for isomerization. The selectivity curves shown in Fig. 8 were determined by placing the same mass (0·2 g) of each catalyst in the reactor. Whatever the support, the amount of isomers was low. The maximum in x_{iso} occurred at 35–40% overall conversion, instead of 70–80% in ideal hydrocracking, and never exceeded 13%. Thus, cracking takes place very rapidly on the isomerized carbenium ions. The best yield in isoheptanes was found over the NiMo-5·3, but the selectivity curves of the two NiMo-3 catalysts were very close to that of the NiMo-5·3, as were the activity curves. The NiMo-3·9 zeolite was slightly less selective than the previous ones, and the NiMo-17 much less. Thus, within the series of five NiMo zeolites, the selectivity for isomers clearly follows the same order as the hydrocracking activity, i.e.

$$\text{HY-5·3} \cong \text{HY-3} > \text{HY-3·9} \gg \text{HY-17}.$$

Influence of support acidity. The rate constants for heptane hydrocracking measured at 553 K over the five NiMo zeolites are given in Table III. The catalysts fall into two categories: the first group comprises the four zeolites with $\text{Si}/\text{Al} = 3$ to 5·3, and the second group solely NiMo-17.

Within the first group, a correlation was found between the rates of heptane hydrocracking and benzene hydrogenation⁹, suggesting that hydrocracking was controlled by the hydrogenation function of the catalyst. Indeed, the NiMo/HY catalysts appear much less active than the Pt/HY, although the activation energies measured here (135 kJ mol^{-1}) lie exactly between the values reported^{10,19} for hexane and octane over Pt/HY. In fact, the rate of hydrocracking was nearly constant within the first four NiMo zeolites, probably because they had equivalent hydrogenation capacities.

Yet the supports had rather different aluminium contents (Table I). The numbers of framework aluminium were determined from the positions of the asymmetric T-O stretching²⁰ in the IR spectrum of the used catalysts. In the first group, they

varied from 29 to 13 Al(F)/u.c. (Table III). The amounts of extra-framework aluminium could then be calculated; they were quite large, and the IR of adsorbed pyridine confirmed that all catalysts bore many acid sites, both Brønsted and Lewis (Table I). Hence, their acidic function is likely to be predominant over the hydrogenation function. As the activity of cracking catalysts is usually related with Al(F), turnover frequencies may be derived upon dividing the hydrocracking rate constants, k , by the appropriate values of Al(F) per unit mass. These turnover numbers (TOF) show greater variations than the rates themselves (Table III), and a maximum TOF appears at about 10 Al(F)/u.c. Such a maximum is frequently encountered in zeolite catalysis, but in the present case, it may not reflect the real acid strength since the reaction was not limited by the acidic function.

This was confirmed by the evolution of selectivities, which ran parallel to the activities. A low yield of isomers means that the desorption of the branched carbenium ions by the C₇ alkene is slow due to an insufficient concentration of n-heptene. In the series of zeolites with the same NiMo loading, the hydro-dehydrogenation activity is presumed constant, so that a large number of acid sites simply decreases the selectivity into isomers.

The NiMo-17 is about ten times less active than the other NiMo zeolites for heptane conversion, and has a poor selectivity for hydroisomerization (Fig. 8). In benzene hydrogenation however, this catalyst was found more active than any other in the MeS/HY series⁹, and from the very low Al(F), a better balance between the metallic and acidic functions was anticipated. The low rate of heptane conversion suggests that hydrocracking is no longer limited by the dehydrogenation of heptane, but is still far from ideal. Two effects contribute to the low selectivity of this catalyst. Firstly, the high reaction temperature favors cracking at the expense of isomerization. Secondly, the average distance between metallic and the few acid sites is rather large, which means a longer pathway for heptenes to be able to desorb the branched carbenium ions as C₇ isomers. This means that the metal sulfide is not very well dispersed. Such transport limitations are also suggested by the lower activation energy (115 kJ mol⁻¹) measured on the NiMo-17 catalyst.

CONCLUSIONS

The NiMo/HY zeolites are characterized by good hydrocracking activities under a high hydrogen pressure. The mechanism is bifunctional, as isomerization precedes cracking. The cracking activities are in line with the amount of Brønsted rather than Lewis sites. The reaction is limited by the rate of hydro-dehydrogenation, as shown by the low yield of heptane isomers. Best activities and selectivities are found at intermediate Si/Al. Selectivity decreases with increasing reaction temperature.

We thank the Ministry of Research and Technology (Paris) for financial help, and Drs C. Marcilly and P. Dufresne (IFP, Rueil) for helpful discussions.

REFERENCES

1. Weitkamp J. in: *Hydrocracking and Hydrotreating* (J. W. Ward, Ed.), A. C. S. Symp. Ser. 20, 1 (1975).
2. Martens J. A., Jacobs P. A., Weitkamp J.: *Appl. Catal.* 20, 239 (1986).
3. Franck J. P., El Malki M., Montarnal R.: *Rev. Inst. Fr. Pet.* 38, 211 (1981).
4. Guisnet M., Alvarez F., Giannetto G., Perot G.: *Catal. Today* 1, 415 (1987).
5. Döhler W. in: *Proc. 8th Int. Congr. Catal.*, Berlin 1984., Vol. III, p. 499. Verlag Chemie, Weinheim 1984.
6. Yan T. Y.: *Ind. Eng. Chem. Res.* 29, 1995 (1990).
7. Dufresne P., Marcilly C.: U.S. 4738940 (1988).
8. Leglise J., Janin A., Lavalley J. C., Cornet D.: *J. Catal.* 114, 388 (1988).
9. Leglise J., El Qotbi M., Goupil J. M., Cornet D.: *Catal. Lett.* 10, 103 (1991).
10. Dufresne P., Quesada-Perez A. M., Mignard S. in: *Catalysis in Petroleum Refining* (D. L. Trimm, Ed.), p. 301. Elsevier, Amsterdam 1989.
11. Bachelier J., Tilliette M. J., Duchet J. C., Cornet D.: *J. Catal.* 87, 292 (1984).
12. Ezzamarty A., Catherine E., Cornet D., Hémidy J. F., Janin A., Lavalley J. C., Leglise J., Meriaudeau P. in: *Proc. 8th Int. Zeolite Conference, Amsterdam, July 1989* (P. A. Jacobs and R. A. van Santen, Eds), p. 1025. Elsevier, Amsterdam 1989.
13. Giannetto G. E., Perot G., Guisnet M.: *Ind. Eng. Chem., Prod. Res. Dev.* 25, 481 (1986).
14. Baltanas M. A., Vansina H., Froment G. F.: *Ind. Eng. Chem., Prod. Res. Dev.* 22, 531 (1983).
15. Vasquez I., Escardino A., Aucejo A.: *Ind. Eng. Chem., Res.* 27, 2039 (1988).
16. Weitkamp J.: *Ind. Eng. Chem., Prod. Res. Dev.* 21, 550 (1982).
17. Corma A., López Agudo A., Nebot I., Tomás F.: *J. Catal.* 77, 159 (1982).
18. Leglise J., Goupil J. M., Cornet D.: *Appl. Catal.* 69, 33 (1991).
19. Ribeiro F., Marcilly C., Guisnet M.: *J. Catal.* 78, 267 (1982).
20. Spiridinova N. L., Spiridinov S. E., Khadjiev S., Machinskaia M. E., Kosolapova A. P.: *Kinet. Katal.* 30, 1005 (1980).